

An exposed cross-section of late Hercynian upper and intermediate continental crust in the Sila nappe (Calabria, southern Italy)

ALFREDO CAGGIANELLI^{1*} and GIACOMO PROSSER²

¹ Dipartimento Geomineralogico - Università di Bari, I-70125 Bari, Italy

² Dipartimento di Scienze della Terra - Università della Basilicata, I-85100 Potenza, Italy

Submitted, December 2000 - Accepted, June 2001

ABSTRACT. — Upper to intermediate levels of continental crust, as shaped by Late Hercynian metamorphism and magmatism, are exposed in the Sila nappe (Calabria, S. Italy) after Tertiary tectonics. Direct observation of the crustal section reveals a composite metamorphic block dominated by low- to high-grade metapelites and meta-arenites, intruded centrally by granitoids. The average thickness of granitoids, estimated on cross-sections and by geobarometry, reaches 9 ± 2 km. Their composition changes with depth from leucogranite to tonalite with increasing colour index. The estimated bulk composition of the Sila nappe is characterised by higher contents of Al_2O_3 , REE and Th and lower contents of CaO and Sr than is typical of upper continental crust, reflecting abundant metapelite in the Sila nappe. Comparisons between metasedimentary rocks from the upper and intermediate levels indicate that intracrustal differentiation was determined by anatexis, which favoured Al_2O_3 , REE and Th enrichment in medium- to high-grade metapelites. Distribution of REE, Th and Zr was connected to the fate of monazite and zircon during crustal anatexis. Melting reactions involved mainly muscovite whereas biotite, enclosing most accessory phases, often remained stable in the residue. Consequent passive enrichment of Th in medium- to high-grade restitic

metapelite determined an unusual increase in radiogenic heat production with depth. Compositional data suggest a connection between leucogranite genesis and anatexis of intermediate crust. The composition of leucogranites is similar to that of crustal melts generated by muscovite dehydration melting reactions. The extremely low concentrations of Sr and Ba and high Rb contents are comparable with those of Himalayan leucogranites.

RIASSUNTO. — L'Unità della Sila (Calabria) rappresenta un blocco di crosta continentale superiore e intermedia tardo ercinica, portato in superficie per effetto della tettonica Terziaria. L'osservazione diretta della sezione crostale consente di descrivere un'unità metamorfica composta intrusa nella parte centrale da granitoidi. Lo spessore medio dei granitoidi stimato per mezzo delle sezioni geologiche e con la geobarometria è di 9 ± 2 km. La composizione dei granitoidi varia con la profondità da leucogranito a tonalite. Tra le rocce metamorfiche risultano prevalenti metapeliti e metaareniti di grado metamorfico da basso ad alto. La composizione globale dell'Unità della Sila è caratterizzata da contenuti elevati di Al_2O_3 , terre rare e Th e da bassi contenuti di CaO e Sr rispetto alla composizione tipica della crosta continentale superiore. Queste differenze sono attribuite all'abbondanza delle metapeliti nella sezione considerata. Un confronto tra i metasedimenti di

*Corresponding author, E-mail: caggianelli@geomin.uniba.it

crosta superiore ed intermedia dell'Unità della Sila rivela che la differenziazione della crosta è avvenuta principalmente attraverso processi di fusione parziale. Questi hanno determinato arricchimento in Al_2O_3 , terre rare e Th nelle metapeliti di medio-alto grado. La distribuzione di terre rare, Th e Zr appare legata alla sorte di monazite e zirconio durante l'anatessi. Le reazioni di fusione parziale hanno coinvolto principalmente la muscovite, mentre la biotite è rimasta generalmente stabile. I minerali accessori, inclusi nella biotite, sono quindi rimasti intrappolati nel residuo. L'abbondanza di monazite ed il conseguente arricchimento in Th nelle metapeliti restituisce quindi un aumento non comune della produzione di calore radiogenico all'aumentare della profondità nella sezione di crosta. Dall'esame dei dati compositivi si possono ipotizzare connessioni tra la genesi dei leucograniti e la fusione parziale della crosta intermedia. La composizione dei leucograniti è simile a quella di fusi cristallini generati attraverso reazioni di disidratazione della muscovite. Le concentrazioni estremamente basse in Sr e Ba e gli elevati contenuti in Rb sono comparabili con quelli dei leucograniti Himalayani.

KEY WORDS: *Continental crust, crustal differentiation, radiogenic heat production, leucogranite.*

INTRODUCTION

The nature and composition of bulk continental crust may be defined using both direct and indirect methods (Taylor and McLennan, 1985; Condie, 1989; Rudnick, 1995). Exhumation of crustal blocks in collisional settings (Fountain and Salisbury, 1981), owing to compressional or late extensional tectonics (e.g. Boundy *et al.*, 1996), sometimes offers the possibility of directly observing various levels of metamorphic and plutonic continental crust (Percival, 1988) and of gaining information on differentiation processes. Within this framework, the final exhumation of crustal rocks is unrelated to metamorphism and plutonism, and is connected with a later tectonic cycle (Ellis, 1987; Bohlen, 1991).

Exhumation of Hercynian crustal blocks is well documented in both northern and

southern Calabria (fig. 1) and took place after Tertiary tectonics (Schenk, 1989; Thomson, 1994). Therefore, the cross-sections exposed in Calabria provide a fine opportunity for direct study of the composition and differentiation of continental crust. Previous works focused on the lower portion of the continental crust exposed in the Serre massif in southern Calabria. Schenk (1981) emphasised important similarities in the lithological sequences and tectonic evolution of the lower crustal cross-sections in the Ivrea zone and the Serre massif, both belonging to the former margin of the Adriatic microplate. Emmermann and Schenk (1989) and Caggianelli *et al.* (1991) gave an account of the composition of lower crustal rocks exposed in the Serre massif and examined the connection between crustal differentiation and granitoid genesis.

In the present paper, attention focuses on the Sila nappe crustal section, exposed in northern Calabria. The crustal section, tilted NE, consists of a composite metamorphic block intruded centrally by granitoids. In this study, 55 samples were collected along a NE-SW transect across the Sila Massif, from the upper to intermediate structural levels of continental crust, and analysed for major and trace element compositions. For samples in appropriate positions in the cross-section, thermobarometry was performed to constrain crustal profiles.

The collected data provide information useful for outlining a general picture of the upper to intermediate continental crust exposed in the Sila nappe. In addition, data and considerations are given on the thickness of the granitoids, intracrustal differentiation, and radiogenic heat production.

GEOLOGICAL SETTING

Together, the massifs of Calabria and the Peloritani Mountains delineate a curved mountain belt linking the NW-SE trending southern Apennines with the E-W trending Maghrebian chain of Sicily (Amodio-Morelli *et al.*, 1976; fig. 1). In contrast to adjoining chains,

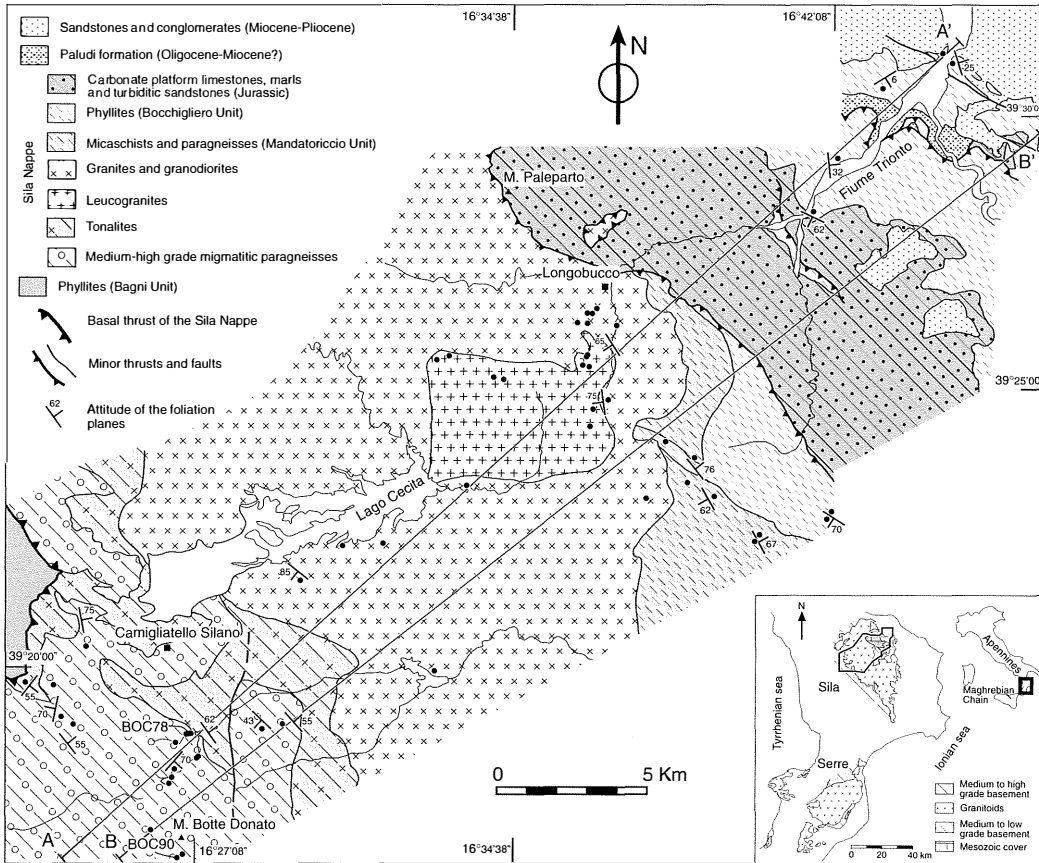


Fig. 1 – Geological sketch-map of Sila massif transect, based on new field observations and literature data (Burton, 1971; Lorenzoni and Zanettin Lorenzoni, 1983). Dots: location of analysed samples. BOC78 and BOC90, respectively, leucogranodiorite and quartz norite samples quoted in text.

dominated by sedimentary rocks, Calabria and the Peloritani Mountains largely consist of pre-Mesozoic crystalline basement units, remnants of a Hercynian chain embodied in the Alpine-Apennine orogen of the western Mediterranean. In Northern Calabria, basement units were stacked over ophiolitic oceanic slices and residues of a Mesozoic to Cenozoic sedimentary cover (see Bonardi *et al.*, in press, for a review). Basically, the tectonic edifice in northern Calabria consists of three levels (Alvarez, 1976; Amodio-Morelli *et al.*, 1976). The lower level includes the tectonic units of the southern Apennines, essentially made up of

meta-carbonates and phyllites of Triassic to Tertiary age. The intermediate level consists of tectonic units derived from Jurassic to Cretaceous oceanic crust. Both are affected by blueschist and greenschist facies Alpine metamorphism (Piccarreta, 1972). The upper level includes three continental crust nappes. The Sila nappe (Dubois, 1976) is a fragment of the Late Hercynian crust comprising low- to high-grade metamorphic rocks intruded by abundant granitoids. It is the highest tectonic unit of the edifice and is the object of this study.

During the Alpine/Apennine orogeny, the Sila nappe overthrust low- and medium-

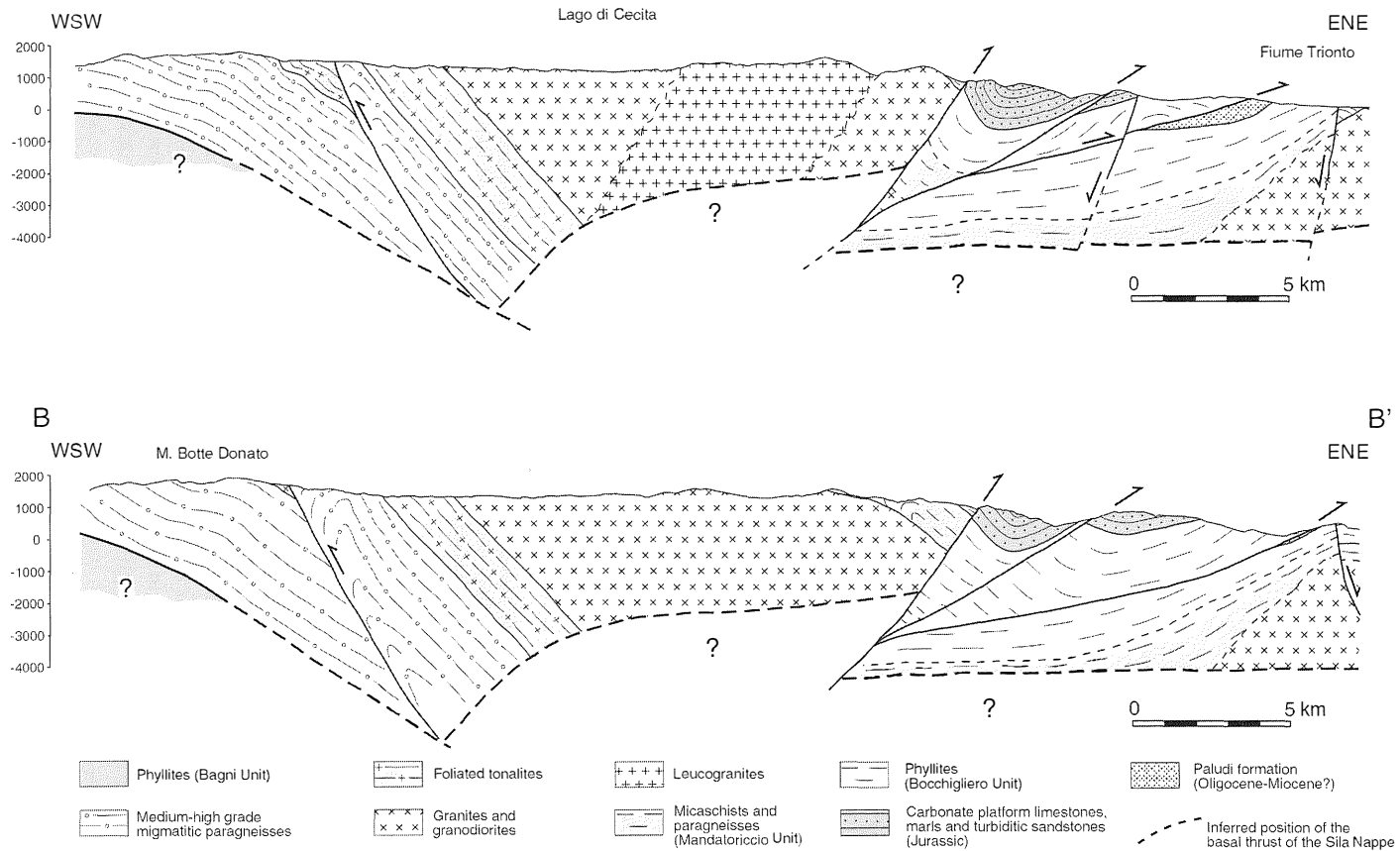


Fig. 2 – Geological cross-sections across Sila nappe. Base is approximately indicated according to available geophysical data (Van Dijk *et al.*, 2000). Basal thrust crops out just NE of cross-section traces (fig. 1). Lines: approximate main foliation in metamorphic and intrusive rocks and bedding planes in sedimentary rocks.

grade basement nappes. Contractional deformation only slightly modified the original Hercynian structure, apart from some minor thrusts in the north-eastern part of the transect (fig. 1). The final exhumation took place from the Oligocene to the Miocene, and is attributed by Thomson (1994) to Apennine late orogenic phases, which tilted the tectonic units north-east. Consequently, deep levels of the crust are now exposed to the south-west near the basal thrust.

CONTINENTAL CRUST EXPOSED IN SILA NAPPE

A simplified profile of continental crust represented in the Sila nappe may be subdivided into three main levels (figs. 1, 2), as earlier described by Dubois (1971).

The upper level, consisting mainly of the Bocchigliero and Mandatoriccio complexes, includes phyllite, micaschist, quartzite and paragneiss with minor amounts of metavolcanic rocks and marble (Borghi *et al.* 1992; Acquafredda *et al.*, 1994). Datings of 326 to 330 Ma by the Rb-Sr whole rock isochron method are considered to represent the age of regional metamorphism (Acquafredda *et al.*, 1991, 1992a). Metamorphic conditions recorded in the Mandatoriccio complex are temperatures of ca. 550-600°C and pressures lower than 400 MPa (Borghi *et al.*, 1992). Both these complexes were later affected by contact metamorphism, due to intrusion by granitoids.

The intermediate level is represented by Carboniferous granitoids with composition varying from leucogranite to tonalite and minor norite (see also Ayuso *et al.*, 1994; Caggianelli *et al.*, 1994). The granitoids are generally peraluminous, with common muscovite. In addition, andalusite, sillimanite or both are generally present in leucogranite, together with sporadic cordierite. The age of the granitoids, determined by Ayuso *et al.* (1994) applying the $^{40}\text{Ar}/^{39}\text{Ar}$ method on hornblende and muscovite and by Gräßner (1999) by the U-Pb method on zircon and monazite, ranges from 289 to 304

Ma. Foliated tonalite together with minor quartz norite are widespread near the contact with the migmatitic paragneiss and, generally, the colour index tends to increase towards lower crustal levels. Leucogranite crosscuts the other granitoids. The contact between granitoids and overlying phyllite is sharp and blocky (Clarke, 1992). Contact metamorphism produced cordierite + andalusite \pm sillimanite hornfels. The lower contact between tonalite and underlying migmatitic paragneiss is gradational (Clarke, 1992). Here, contact effects are revealed by more widespread migmatization, probably enhanced by fluids released by crystallising tonalitic magmas. Near the border zone, the tonalite contains garnet and/or muscovite, owing to contamination with wall rock.

The lower level, belonging to the former Mt. Gariglione complex (Amodio-Morelli *et al.*, 1976), is largely made up of migmatitic paragneiss with minor lenses of metabasite and marble (Gräßner, 1999). Migmatitic paragneiss consists of quartz, feldspars, biotite, muscovite, sillimanite, garnet, cordierite \pm andalusite \pm hercynite (gahnite up to 30%). The amount of leucosome is extremely variable. Peak metamorphism in the basal part, dated at 302-304 Ma by the U-Pb method on monazite, reached a temperature of ca. 770°C and a pressure of ca. 600 MPa. After peak metamorphism, high-grade rocks underwent decompression of 120 MPa and then slow near-isobaric cooling (Gräßner, 1999; Gräßner *et al.*, 2000).

ESTIMATE OF THICKNESS OF GRANITOID

A first estimate of granitoid thickness may be obtained by examining the geological cross-sections of fig. 2. Estimates are constrained by the attitude of contacts and the assumption of the absence of faults in the central part of Sila, where rock outcrops are rare and of modest vertical extent. With these limiting considerations, a granitoid thickness varying from 9 to 11 km may be estimated.

TABLE 1
Selected compositions of mineral phases from hornfels and migmatitic paragneiss.

	Ms	Hornfels		Pl	Bt	Migmatitic paragneiss		Pl
		Bt	Crd			Crd	Grt	
SiO ₂	46.1	35.1	47.8	63.8	34.6	46.8	37.1	59.1
TiO ₂	1.36	2.67	n.d.	n.d.	2.61	n.d.	0.12	n.d.
Al ₂ O ₃	36.72	21.19	33.88	22.96	20.54	33.44	22.04	26.18
FeO	0.81	19.77	8.84	0.20	20.75	9.41	33.40	0.20
MnO	n.d.	n.d.	0.22	n.d.	n.d.	0.15	1.60	n.d.
MgO	0.53	8.71	7.53	n.d.	8.82	8.22	5.10	n.d.
CaO	n.d.	n.d.	n.d.	2.36	n.d.	n.d.	0.99	6.30
Na ₂ O	1.1	n.d.	n.d.	10.4	n.d.	n.d.	n.d.	8.1
K ₂ O	9.52	8.24	n.d.	n.d.	8.87	n.d.	n.d.	n.d.
<i>tot</i>	96.14	95.68	98.27	99.72	96.19	98.02	100.35	99.88
Si	6.04	5.27	4.94	2.82	5.23	4.87	2.94	2.64
Ti	0.13	0.30			0.30		0.01	
Al ^{IV}	1.96	2.73	1.06	1.20	2.77	1.13	0.06	1.38
Al ^{VI}	3.72	1.02	3.06		0.89	2.97	2.00	
Fe	0.09	2.48	0.76	0.01	2.62	0.82	2.22	0.01
Mn			0.02			0.01	0.11	
Mg	0.10	1.95	1.16		1.99	1.28	0.60	
Ca				0.11			0.08	0.30
Na	0.28			0.89				0.70
K	1.59	1.58			1.71			
Σ O	22	22	18	8	22	18	12	8
Σ cat	13.91	15.33	11.00	5.03	15.51	11.08	8.02	5.03
Mg/(Mg+Fe)	0.53	0.44	0.60		0.43	0.61	0.21	

n.d. = not detected. Analyses performed on a Cambridge S360 SEM equipped with a LINK AN 10000 ED detector (CNR, Chimica dei Plasmi, Dip. Geomineralogico, University of Bari). Operating conditions: 15 kV accelerating potential, 1 nA probe current. Standardisation: several minerals and pure compounds from Micro-Analysis Consultants Ltd.

To obtain an independent check, thermobarometry was performed on selected samples. The basic assumptions were:

1) Emplacement of granitoids took place in a narrow time span; available geochronological data indicate that this event occurred between 305 and 290 Ma (Ayuso *et al.*, 1994; Gräßner, 1999; Gräßner *et al.*, 2000).

2) Peak metamorphism in both roof hornfels and bottom wall rocks was reached owing to the heat released by crystallising granitoid magmas. This may be obvious for the roofing hornfels, but is more dubious for the

migmatitic paragneiss below. Recent U-Pb dates on zircon and monazite from metamorphic and granitoid rocks (Gräßner, 1999; Gräßner *et al.*, 2000) pointed out a close match in the timing of metamorphism and the intrusion of granitoids. Metamorphic zircon ages range from 296 to 305 Ma, overlapping those for peraluminous granites (298-304 Ma). U-Pb monazite ages are 302-304 Ma for both the metamorphism of migmatitic paragneiss and granitoid intrusion. Gräßner (1999) considered these data as strong evidence in favour of a cause-effect connection between

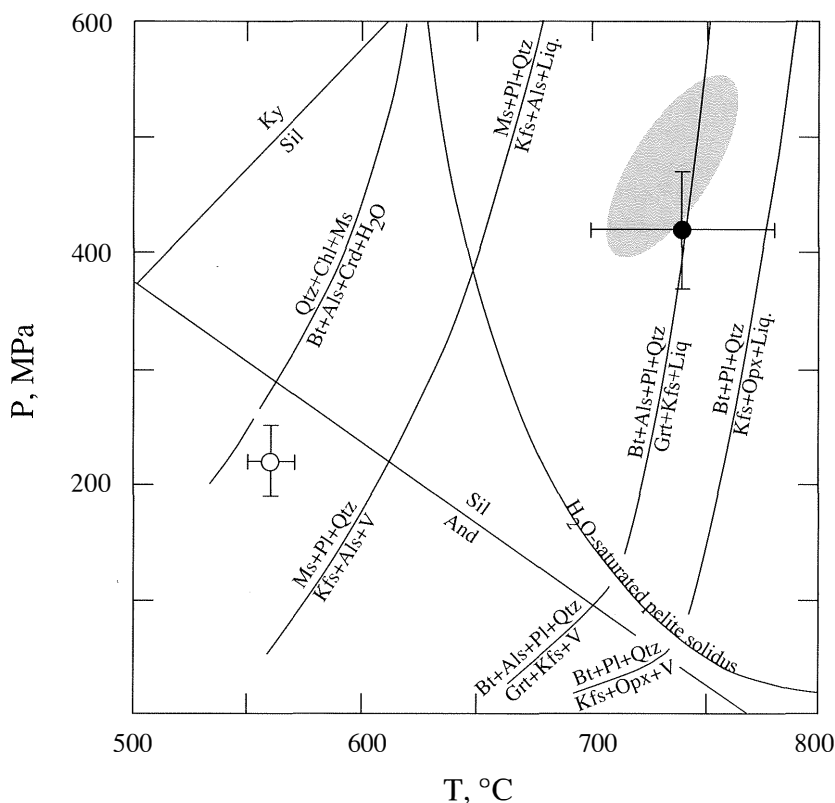


Fig. 3 – P-T diagram showing estimated peak metamorphic conditions for metapelites at roof (open circle) and bottom (closed circle) of granitoids. Shaded area: peak estimates in Sila high-grade metapelites according to Gräßner *et al.* (2000). And=Sil and Sil=Ky lines from Holdaway (1971). Chlorite-out reaction, H₂O-saturated pelite solidus and approximate positions of muscovite and biotite dehydration reactions following Pattison and Tracy (1991) and Spear (1993).

plutonism and metamorphism, as generally proposed for low-pressure metamorphic belts (Lux *et al.*, 1986).

With these assumptions, geobarometry was performed to calculate granitoid thickness. Minerals in hornfels above the intrusions and in the migmatitic paragneiss below were analysed by SEM-EDS (Table 1). Muscovite + quartz + biotite + andalusite + cordierite ± fibrolite assemblages in the hornfels indicate equilibrium at 220 MPa and 560°C (fig. 3), using thermodynamic data from Holland and Powell (1998). Thus, the depth of the top of the granitoids at the time of metamorphism was about 8 km. Instead, for migmatitic paragneiss characterised by garnet + cordierite +

sillimanite + quartz + plagioclase assemblages, application of garnet - cordierite thermometry and garnet - cordierite - sillimanite - quartz barometry (Nichols *et al.*, 1992) indicates equilibrium at T = 740°C and P = 420 MPa (fig. 3). The metamorphic evolution of the migmatitic paragneiss has recently been studied by Gräßner (1999). Peak estimates on the top of the migmatitic paragneiss indicate 740°C, with pressures varying from 400 to 440 Mpa. Application of the hornblende - plagioclase thermobarometer (Anderson and Smith, 1995; Holland and Blundy, 1994) on tonalite adjacent to migmatitic paragneiss provided T and P estimates for late magmatic crystallisation of 707 ± 40°C, and 490 ± 60 MPa, respectively

(Caggianelli *et al.*, 1997). Lastly, a pressure of 400 MPa has been suggested for the genesis of olivine - plagioclase corona textures in norite and for the neighbouring migmatitic paragneiss (Acquafredda *et al.*, 1992b). Therefore, the original position of the bottom of the granitoids is set at a depth of 15 to 17 km.

From these data, the estimated thickness of the granitoids ranges from 7 to 9 km, i.e., slightly lower than the values obtained from the geological cross-sections. This difference may

be due either to assumptions on the dip angle of the contacts or to faults in the central part of the section.

COMPOSITION OF UPPER AND LOWER METAMORPHIC LEVELS

The metamorphic rocks exposed in the Sila nappe derive mostly from protoliths of pelitic to arenitic composition. Meta-igneous rocks are

TABLE 2
Average composition of main rock units (columns 1-6) crossed by geological sections and of minor rock types (columns 7-12).

	main rock types						minor rock types					
	1	2	3	4	5	6	7	8	9	10	11	12
wt%												
SiO ₂	62.94	64.74	73.42	68.92	53.70	56.72	84.44	70.11	44.35	46.09	72.94	72.79
Al ₂ O ₃	17.50	18.24	13.97	15.47	18.52	21.01	7.34	15.79	29.59	16.61	13.96	14.20
Fe ₂ O ₃	6.47	6.56	1.36	3.30	8.12	9.62	2.35	1.94	15.73	10.72	2.56	1.46
MnO	0.06	0.06	0.02	0.05	0.11	0.12	0.02	0.02	0.22	0.20	<0.01	0.01
MgO	2.44	1.78	0.23	0.97	4.88	3.17	0.61	0.54	4.89	9.98	0.61	0.19
CaO	0.55	0.49	0.29	1.50	6.88	1.49	0.50	2.29	0.11	13.63	0.16	0.50
Na ₂ O	1.94	1.20	3.16	3.22	1.72	1.34	1.06	3.95	0.28	0.93	2.80	2.40
K ₂ O	3.05	3.52	5.25	3.86	2.18	2.65	1.42	3.09	0.29	0.60	4.16	6.22
TiO ₂	0.82	0.87	0.09	0.38	0.98	1.22	0.45	0.28	2.07	0.98	0.32	0.16
P ₂ O ₅	0.12	0.13	0.13	0.17	0.21	0.10	0.08	0.09	0.38	0.03	0.18	0.15
LOI	3.23	2.29	0.97	1.23	1.48	1.73	1.73	0.64	1.90	1.10	1.71	0.97
Tot	99.12	99.90	98.91	99.08	98.78	99.17	100.02	98.74	99.81	100.87	99.41	99.05
ppm												
Sc	18	17	3	7	27	24	8	3	21	38	6	4
Be*	3	2	1	2	2	3	1	<1	8	<1	2	<1
V*	115	106	5	36	169	163	50	12	304	201	24	<5
Co	15	15	4	6	19	24	7	7	47	61	5	3
Ni*	35	32	<15	<15	30	53	<15	<15	176	363	<15	16
Cu*	25	13	<10	<10	9	11	<10	<10	176	11	<10	<10
Zn*	78	82	15	77	78	115	15	32	244	70	47	<30
Ga	23	24	19	19	20	29	11	17	39	14	20	14
Ge	1.6	1.9	1.5	1.4	1.8	1.8	1.4	0.9	1.3	1.7	1.4	1.5
Rb	135	152	245	153	94	108	74	85	19	7	169	197
Sr	130	85	28	151	214	111	52	512	4	174	110	79
Y	27	32	20	18	23	41	19	7	5	23	30	23
Zr	187	186	52	150	184	263	197	178	374	62	136	27
Nb	11	14	8	9	8	17	7	5	19	2	8	3
Sn*	3	3	4	4	3	<1	2	1	<1	2	5	3
Cs	5.1	8.0	3.5	4.2	3.7	2.7	1.8	1.8	1.7	<0.1	5.4	2.5
Ba	751	300	154	670	689	557	252	1560	28	34	960	270

TABLE 2: *continued*

	main rock types							minor rock types				
	1	2	3	4	5	6	7	8	9	10	11	12
ppm												
La	30.22	42.08	12.56	36.56	21.75	59.04	19.30	32.20	17.90	2.70	17.50	6.80
Ce	58.60	84.00	25.76	68.46	43.30	114.92	42.00	56.20	33.70	6.80	41.00	12.50
Pr	6.42	9.46	3.05	7.76	5.20	12.75	4.95	5.69	3.63	1.11	4.57	1.39
Nd	25.24	37.18	11.89	29.88	21.55	49.29	18.85	20.40	14.40	6.82	18.10	5.30
Sm	4.96	7.34	3.27	5.80	4.62	9.59	3.52	3.69	2.38	2.27	4.04	1.57
Eu	1.12	1.39	0.23	1.03	1.62	1.64	0.85	0.99	0.10	1.09	0.59	0.62
Gd	4.55	6.53	3.17	4.90	4.50	8.43	3.55	2.87	1.91	3.05	3.79	2.00
Tb	0.72	0.97	0.59	0.64	0.67	1.19	0.53	0.38	0.21	0.57	0.74	0.45
Dy	4.33	5.63	3.38	3.34	4.03	6.93	2.99	1.73	0.98	3.87	4.85	3.48
Ho	0.89	1.12	0.62	0.57	0.79	1.40	0.63	0.26	0.17	0.82	1.00	0.72
Er	2.71	3.18	1.84	1.60	2.40	4.25	1.85	0.64	0.60	2.49	2.99	2.34
Tm	0.42	0.47	0.29	0.23	0.32	0.62	0.27	0.07	0.11	0.38	0.47	0.38
Yb	2.67	2.88	1.79	1.34	1.98	3.83	1.70	0.42	0.79	2.30	2.85	2.28
Lu	0.41	0.43	0.26	0.18	0.31	0.58	0.27	0.05	0.19	0.39	0.42	0.36
Σ REE	143.26	202.66	68.71	162.28	113.03	274.47	101.27	125.59	77.07	34.66	102.91	40.19
Hf	5.2	5.3	2.2	4.2	5.1	7.3	5.2	4.6	9.9	1.7	4.1	1.0
Ta	1.0	1.1	1.6	1.0	0.7	1.3	0.7	0.4	1.6	<0.1	0.8	0.3
Tl	0.90	0.89	1.39	0.98	0.58	0.80	0.97	0.55	0.24	0.22	1.21	1.10
Pb*	10	18	20	17	10	13	10	26	<5	<5	25	40
Th	12.4	15.0	8.2	14.6	4.5	20.4	7.4	8.7	6.2	0.6	11.7	3.8
U	3.16	3.06	3.12	2.14	1.38	3.09	1.98	1.60	0.88	0.59	3.71	2.02
Th/U	3.9	4.9	2.6	6.8	3.3	6.6	3.7	5.4	7.1	1.1	3.2	1.9
A**	1.95	2.15	1.91	1.82	0.91	2.75	1.16	1.29	0.77	0.27	2.14	1.30

1) phyllite and related hornfels from Bocchigliero complex ($n=4$); 2) micaschist and paragneiss from Mandatoriccio complex ($n=5$); 3) leucogranite ($n=11$); 4) granite and granodiorite ($n=13$); 5) tonalite to quartz norite ($n=3$); 6) migmatitic paragneiss ($n=12$); 7) quartzite ($n=2$); 8) leucogranodiorite (BOC78); 9) Grt-Crd fels; 10) amphibolite; 11) meta-rhyolite; 12) augengneiss. * below detection limits in some samples. ** A: radiogenic heat production in $\mu\text{W}/\text{m}^3$. Decay energies of K, Th and U from Philpotts (1990). Density values set to $2700 \text{ kg}/\text{m}^3$, except for mafic and garnet-rich rocks, for which a value of $3000 \text{ kg}/\text{m}^3$ is adopted.

Analytical methods for rock analyses.

55 rock samples (see map in fig. 1 for location) were selected for chemical analyses, performed by ICP at Actlabs. Rock powders underwent lithium metaborate/tetraborate fusion and were analysed by ICP-AES for major oxides, Sc and Be, and ICP-MS for all other trace elements. Single analyses may be obtained from authors upon request.

represented in minor amounts, and their composition is described in the last part of this section.

Among metasedimentary rocks, metapelite is abundant, with smaller amounts of meta-arenite and meta-siltstone. The following rock types were recognised (Table 2): *a*) very low- to low-grade phyllite with related hornfels (Bocchigliero complex); *b*) medium-grade

micaschist and paragneiss (Mandatoriccio complex); *c*) quartzite (Bocchigliero and Mandatoriccio complexes); *d*) migmatitic paragneiss (former Mt. Gariglione complex); *e*) Grt-Crd fels (former Mt. Gariglione complex).

The diagram of Herron (1988) (fig. 4) indicates that most samples fall in the field of shale. Remarkable exceptions are represented

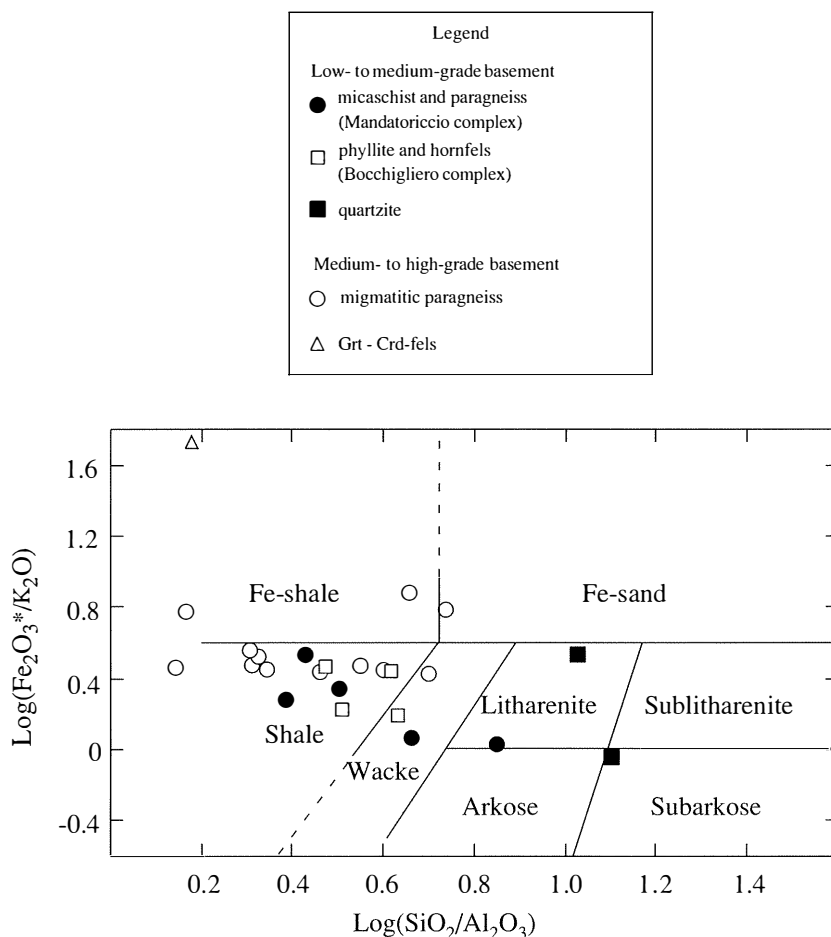


Fig. 4 – Compositional features of metasedimentary rocks of Sila nappe crustal section: chemical classification diagram proposed by Herron (1988) for terrigenous sands and shales. Fe_2O_3^* = all Fe expressed as Fe_2O_3 .

by the Grt-Crd fels, characterised by a very high $\text{Fe}_2\text{O}_3^*/\text{K}_2\text{O}$ ratio, and by quartzite and one quartz-rich paragneiss from the Mandatoriccio complex, falling in the field of litharenite and subarkose.

Linear trends with negative correlations characterise the Al_2O_3 , Fe_2O_3^* , MgO and TiO_2 vs SiO_2 scatter diagrams (fig. 5). In the other diagrams scattering of data points is evident. Coarse negative correlations with silica may be deduced only for K_2O , Ba and Rb. The migmatitic paragneiss shows a notable increase

in Al_2O_3 (up to 31%) and decrease in SiO_2 (down to 43 wt%) for samples progressively richer in restite.

With few exceptions, REE patterns (fig. 6) are characterised by similar profiles but variable concentration levels. When compared with the post-Archean Australian Shale (PAAS of Taylor and McLennan, 1985; $[\text{Ce}/\text{Yb}]_N = 7.50$; $\Sigma\text{REE} = 183$ ppm; $\text{Eu}/\text{Eu}^* = 0.65$), phyllite and hornfels turn out to be strikingly alike (averages: $[\text{Ce}/\text{Yb}]_N = 7.40$; $\Sigma\text{REE} = 178$; $\text{Eu}/\text{Eu}^* = 0.72$), except for one phyllite,

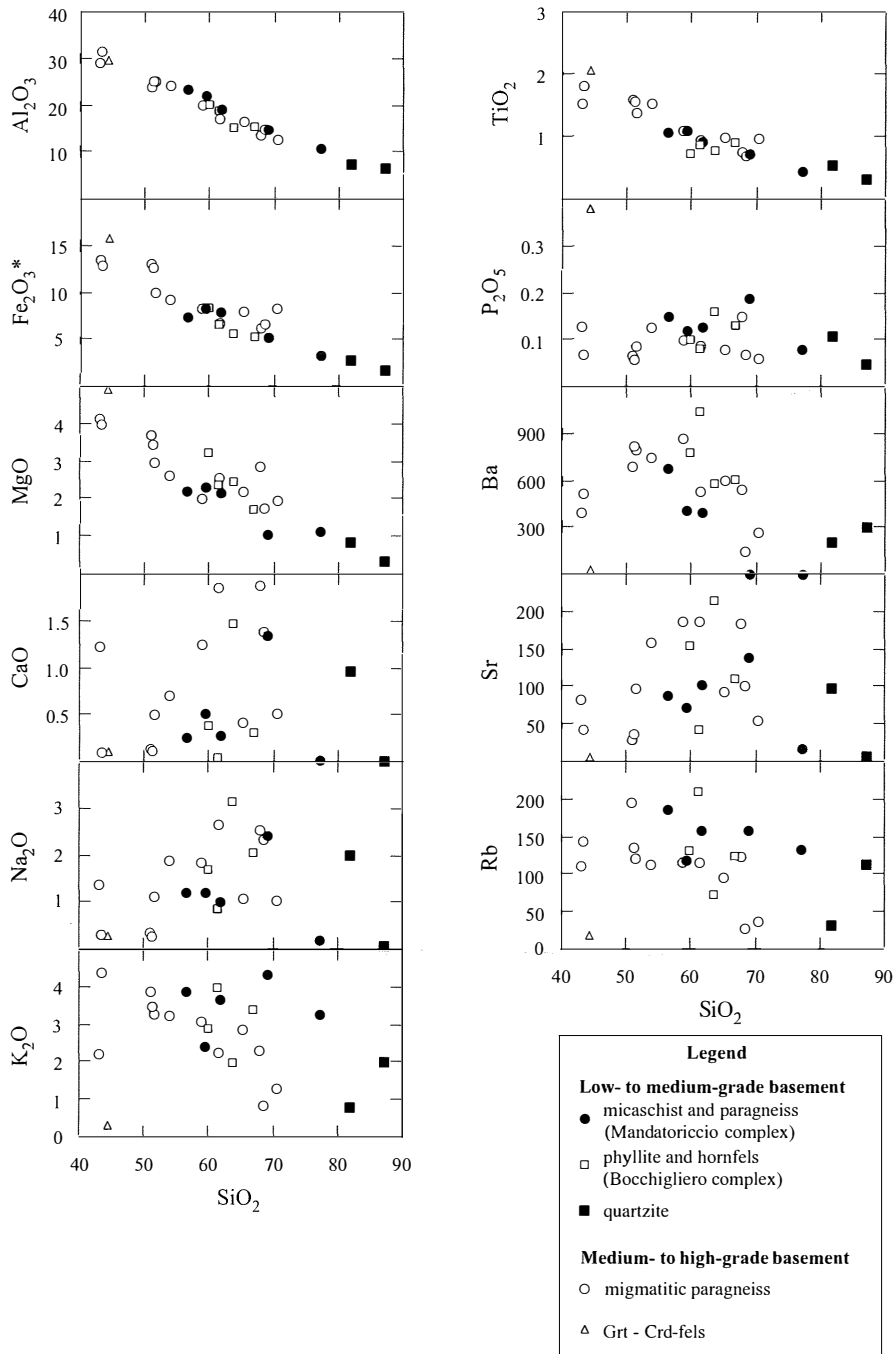


Fig. 5 – Harker diagrams of selected major oxides and trace elements of the metasedimentary rocks in the Sila nappe crustal section. $Fe_2O_3^*$ = all Fe expressed as Fe_2O_3 .

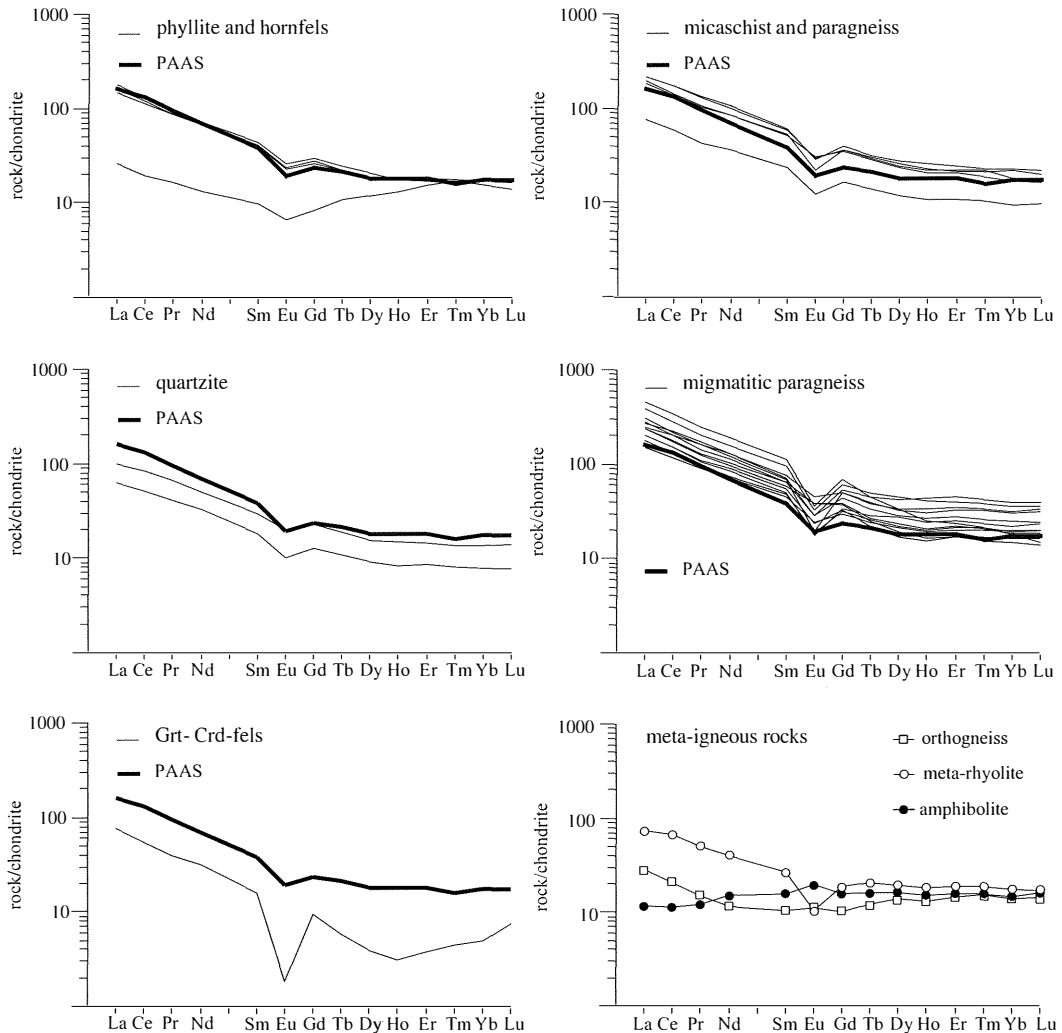


Fig. 6 – REE patterns of metasedimentary and meta-igneous rocks of Sila nappe crustal section. Chondrite normalising values from McDonough and Sun (1995). REE contents in PAAS from Taylor and McLennan (1985).

characterised by an anomalous concave-up pattern with similar concentration levels of LREE and HREE. Micaschist and paragneiss from the Mandatoriccio complex show higher PAAS-like profiles ($[\text{Ce}/\text{Yb}]_{\text{N}} = 7.86$; $\Sigma\text{REE} = 231$ ppm; $\text{Eu}/\text{Eu}^* = 0.61$). Lower levels of REE are observed only in one quartz-rich sample ($\Sigma\text{REE} = 90$ ppm). Quartzite displays patterns

similar to PAAS ($[\text{Ce}/\text{Yb}]_{\text{N}} = 6.51$) and, owing to abundant quartz, lower concentrations of REE ($\Sigma\text{REE} = 101$ ppm).

The migmatitic paragneiss shows a typical post-Archean shale profile ($[\text{Ce}/\text{Yb}]_{\text{N}} = 8.66$) but with weak to strong enrichment in REE ($\Sigma\text{REE} = 288$ ppm) and in most cases a deeper Eu anomaly ($\text{Eu}/\text{Eu}^* = 0.55$). The Grt-Crd fels

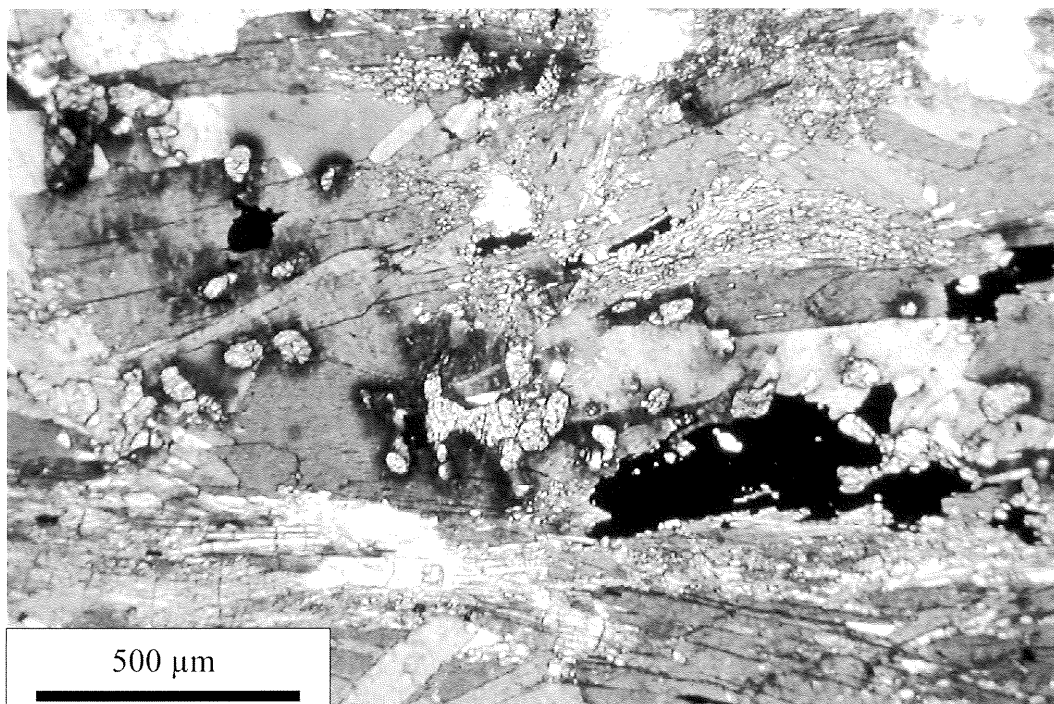


Fig. 7 – Micrograph showing abundance of inclusions in biotite within migmatitic paragneiss. Most inclusions, surrounded by a pleochroic halo, are first represented by monazite and then by zircon.

exhibits a more fractionated pattern ($[Ce/Yb]_N = 11.20$) with lower concentration levels, a pronounced negative Eu anomaly ($Eu/Eu^* = 0.15$) and a marked concave-up profile from Gd to Lu.

REE enrichment observed in most migmatitic paragneiss is linked to the abundance of REE-bearing accessory phases, such as monazite and probably zircon and xenotime. This is in agreement with the abundance and size of these accessory phases in some restitic metapelites (fig. 7). In addition, the remarkable positive correlation between Th and Ce (fig. 8a) is indicative of the strong control of monazite over the distribution of LREE. The wide range of Ce content observed in the migmatitic paragneiss (including the Grt-Crd fels) appears to be positively correlated with K_2O (fig. 8b). In these rocks, biotite is the main reservoir of K_2O and thus this correlation

may be related to positive covariation of monazite and biotite contents. Instead, the role of zircon together with garnet may be important in carrying HREE, since concentration levels of Zr may be high (up to 410 ppm). According to McLennan (1989), Zr concentrations in shales above the critical value of 200 ppm indicate the influence of zircon on the HREE balance. The coarse positive correlation of Zr and Yb observed in the Sila metapelite lends support to this hypothesis (fig. 8c).

Meta-igneous rocks crossed by the transect are represented by amphibolitic lenses, meta-volcanic rocks and augengneiss (Table 2). They derive from pre-Hercynian magmatic protoliths, and their volume proportions in the chosen crustal profile are estimated to be very low. Protoliths of meta-volcanic rocks are Ordovician to Devonian calc-alkaline rhyolite

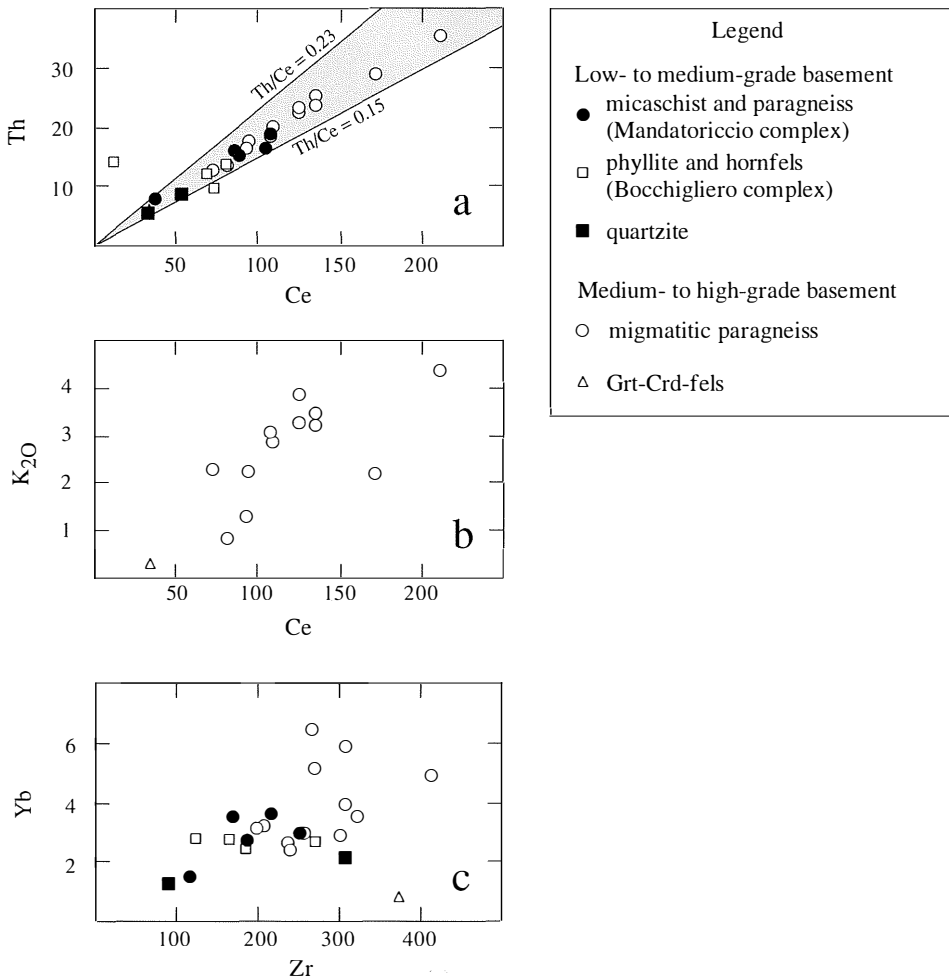


Fig. 8 – a) Th-Ce scatter diagram illustrating role of monazite in LREE distribution in metasedimentary rocks. Shaded area bounded by lines with minimum and maximum Th/Ce ratios detected in monazites from a Calabrian Late Hercynian migmatite. b) K_2O -Ce scatter diagram for medium- to high-grade metasedimentary rocks. Positive covariations of K_2O and Ce may be linked to enrichment in residues of biotite and monazite during anatexis. c) Yb-Zr scatter diagram illustrating possible role of zircon in HREE distribution in metasedimentary rocks.

and andesite interbedded in the Cambrian to Devonian terrigenous sequence of the Bocchigliero complex (Acquafredda *et al.*, 1994). Amphibolite and augengneiss were sampled in the border zone between tonalite and the medium- to high-grade basement. Comparable augengneiss in the Serre massif provided an U-Pb zircon age of 550 Ma, assumed to be a magmatic crystallisation age

(Senesi, 1999). The REE patterns of these minor rock types are shown in fig. 6. The amphibolitic lens shows a flat REE pattern with a weak positive Eu anomaly. The meta-rhyolite sample is characterised by a moderately fractionated pattern and a pronounced negative Eu anomaly. The augengneiss sample reveals negligible fractionation and a weak Eu anomaly.

COMPOSITION OF INTERMEDIATE
GRANITOID LEVEL

Intrusive rocks exposed along the transect include:

a) leucogranite and leucogranodiorite; *b)* granodiorite to granite; *c)* tonalite with minor quartz norite. Compositions are listed in Table 2.

The intrusive rocks show subalkaline affinity (fig. 9a) and follow a calc-alkaline trend (fig. 9b). Except for the quartz norite sample (BOC90), they are characterised by peraluminous composition with an A/CNK molecular ratio greater than 1.1. In the Harker diagrams (fig. 10), excluding the quartz norite point, linear trends and negative correlations are evident for Al_2O_3 , Fe_2O_3^* , MgO, CaO and TiO_2 . A lower correlation with silica or curved trends may be observed in the other diagrams.

Leucogranite is characterised by high K_2O and Rb and low Ba and Sr. Instead, the leucogranodiorite sample (BOC78), coming from a small mass intervening with the migmatitic paragneiss, stands out for its low Rb and high Sr and Ba contents. Closer examination of the Rb and Sr Harker diagrams shows that leucogranite is probably not a differentiation product of the other granitoids. In any case, on the basis of the Rb, Ba and Sr contents, the leucogranite is clearly different from the other granitoids, as is shown in the triangular diagram of fig. 11.

REE patterns (fig. 12) are useful discriminants among granitoid groups. Typical

leucogranite patterns are poorly fractionated ($(\text{Ce}/\text{Yb})_{\text{N}} = 2.91$), with a sharp negative Eu spike ($\text{Eu}/\text{Eu}^* = 0.23$), whereas granite to granodiorite are characterised by fractionated patterns ($(\text{Ce}/\text{Yb})_{\text{N}} = 14.37$), with moderate negative Eu anomalies ($\text{Eu}/\text{Eu}^* = 0.67$). Tonalite and quartz norite display mildly fractionated patterns ($(\text{Ce}/\text{Yb})_{\text{N}} = 7.89$) with negligible or absent Eu anomalies ($\text{Eu}/\text{Eu}^* = 0.97$). Lastly, the leucogranodiorite shows a very fractionated pattern ($(\text{Ce}/\text{Yb})_{\text{N}} = 35.14$) with a negligible Eu anomaly ($\text{Eu}/\text{Eu}^* = 0.93$).

ESTIMATE OF BULK COMPOSITION OF SILA NAPPE

An estimate of the bulk composition of upper and intermediate continental crust exposed in the Sila nappe was attempted by examining the areal proportions of the main rock units crossed in the crustal sections of fig. 2 (Table 3). The obtained proportions and appropriate rock density values were then used to calculate weighted averages (columns 1-6, Table 2). The resulting average compositions (Table 4) reflect the abundance of metapelite in the Sila nappe crustal section. Consequently, Al_2O_3 content is distinctly higher and CaO and Na_2O contents lower than in typical upper crustal averages (Taylor and McLennan, 1985; Condie, 1993). In the incompatible element spider-diagram of fig. 13, a comparison is made with typical upper crust estimates. Major deviations include the higher contents of Th

TABLE 3

Proportions of main rock types estimated on geological cross-sections across Sila nappe.

rock type	Sila nappe section A-A' (fig. 2)	Sila nappe section B-B' (fig. 2)
phyllite and hornfels	0.194	0.220
micaschist and paragneiss	0.092	0.086
leucogranite	0.141	—
granite and granodiorite	0.221	0.321
tonalite to qtz norite	0.091	0.061
migmatitic paragneiss	0.259	0.312

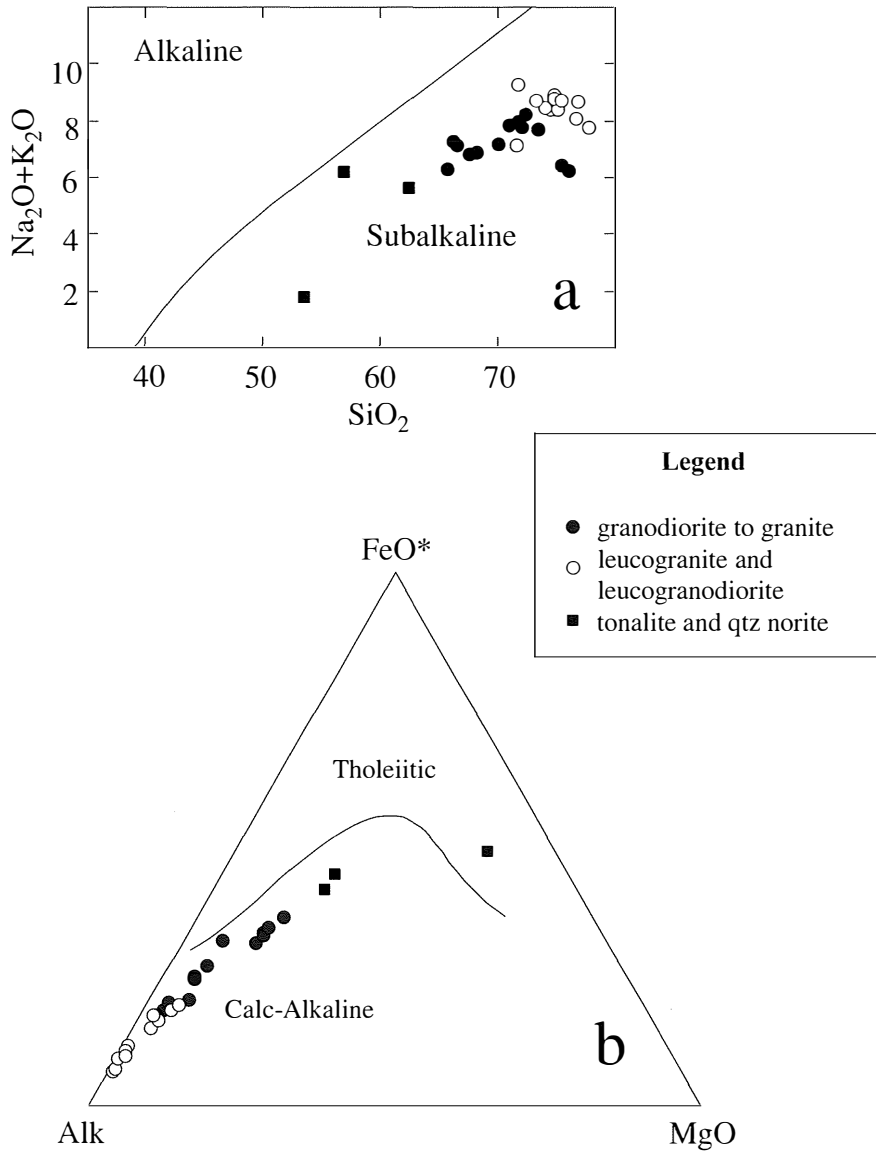


Fig. 9 – Chemical classification of intrusive rocks making up central part of Sila nappe crustal section according to a) Σ Alk - SiO_2 diagram; b) AFM diagram of Irvine and Baragar (1971). In a), analyses are recalculated to 100% after subtraction of H_2O .

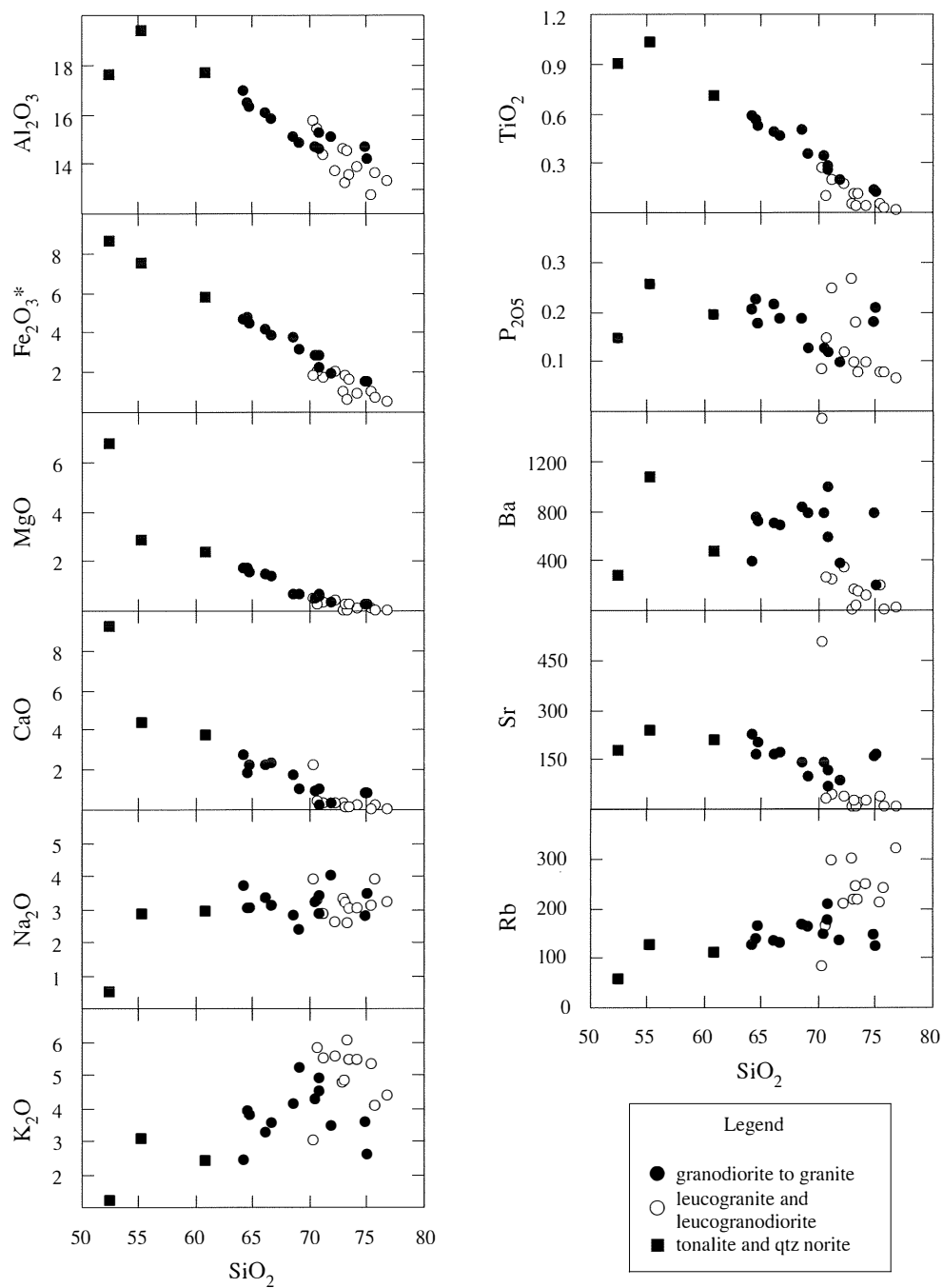


Fig. 10 – Harker diagrams of selected major oxides and trace elements for intrusive rocks of intermediate level of Sila crustal section.

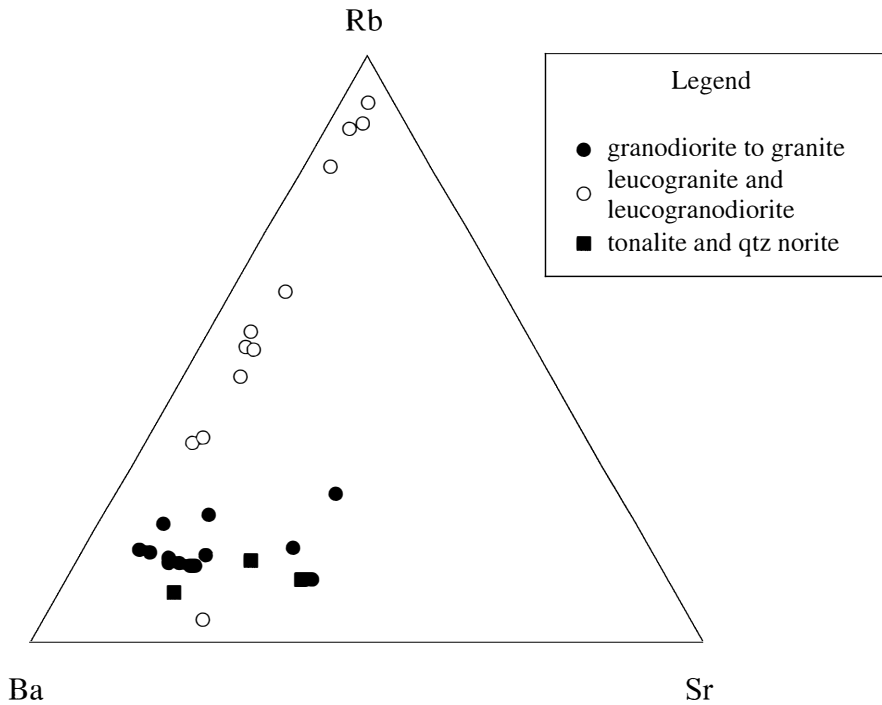


Fig. 11 – Rb-Ba-Sr triangular diagram of intrusive rocks of intermediate level of Sila nappe crustal section.

and LREE in the Sila crust and the distinctly lower Sr. In addition, a comparison with the estimate of Taylor and McLennan (1985) shows more pronounced negative anomalies in Ta and Nb. This fits the estimates of Condie (1993) and Barth *et al.* (2000), which indicate higher concentrations of Nb and Ta (11.5 ± 2.5 and 0.92 ± 0.12 ppm, respectively) in upper continental crust.

RADIOGENIC HEAT PRODUCTION IN SILA NAPPE

Contents of U, Th and K were used to estimate radiogenic heat production in the rocks exposed along the crustal section of the Sila nappe. Decay energies e_i used in calculations, expressed in mW/kg, were the following values reported by Philpotts (1990):

$$\begin{aligned} e_U &: 9.66 * 10^{-2} \\ e_{Th} &: 2.65 * 10^{-2} \\ e_K &: 3.58 * 10^{-6} \end{aligned}$$

Using these constants, U, Th and K concentrations in ppm (c_i) and density values (ρ) in kg/m^3 , radiogenic heat production A was obtained by the following formula:

$$A (\mu\text{W/m}^3) = (\rho \sum e_i c_i) / 1000$$

Values of 1.95 and 2.15 $\mu\text{W/m}^3$ were obtained for the phyllite and micaschist to paragneiss of the upper crust and 2.75 $\mu\text{W/m}^3$ for the migmatitic paragneiss. Granitoid rocks have values of radiogenic heat production ranging from 1.91 to 0.79 $\mu\text{W/m}^3$, with higher values in granite and granodiorite and lower ones in tonalite and quartz norite. These results show that, in metasedimentary rocks, higher

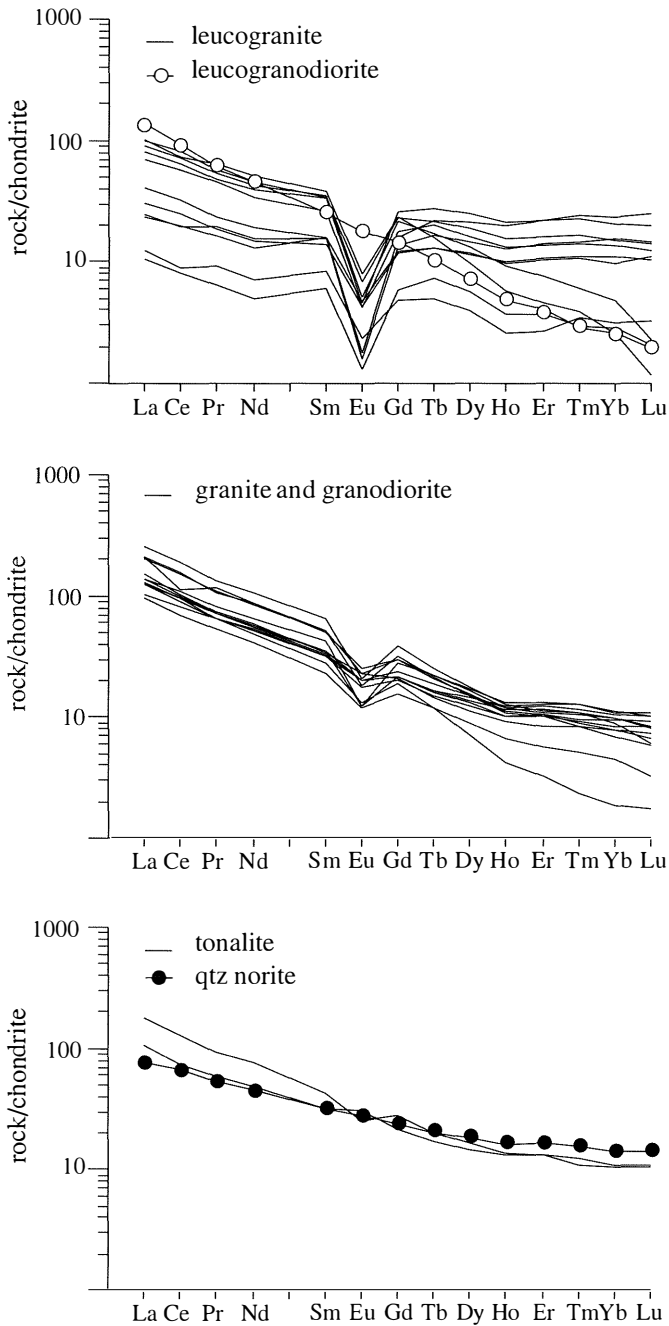


Fig. 12 – REE patterns of intrusive rocks of intermediate level of Sila nappe crustal section. Chondrite normalising values from McDonough and Sun (1995).

heat production characterises the deeper levels of this crustal section. This is contrary to general variations in heat production with depth in old shield areas, implying an exponential decrease of A with depth.

The observed increase in A with depth may be linked to the mode of partial melting of medium- to high-grade metapelite and/or the fast melt segregation rate which prevents

equilibration with the source (Watt *et al.*, 1996). The dominant mechanism responsible for the generation of melts in the Sila metapelite was by dehydration melting reactions involving white mica. Biotite was not significantly involved, with two consequences:

- a) part of the K was left in the residue;
- b) biotite armoured tiny inclusions such as zircon, xenotime and chiefly monazite (fig. 7),

TABLE 4

Composition estimates for Sila nappe Late Hercynian crust, calculated by weighted averages of columns 1-6, Table 2. Weights are rock proportions in Table 3, density values given in footnotes of Table 2. Compositions of Phanerozoic upper continental crust, according to Taylor and McLennan (1985) and Condie (1993), reported for comparison.

	Sila nappe section A-A'	Sila nappe section B-B'	av. anhydrous composition	upper crust ¹	upper crust ²
wt%					
SiO ₂	63.11	62.30	64.52	66.00	65.69
Al ₂ O ₃	17.69	18.17	18.45	15.20	15.15
Fe ₂ O ₃	6.12	6.65	6.57	4.95	5.47
MnO	0.07	0.08	0.08		
MgO	2.19	2.32	2.32	2.20	2.24
CaO	1.55	1.54	1.59	4.20	3.70
Na ₂ O	2.12	2.06	2.15	3.90	3.32
K ₂ O	3.37	3.15	3.36	3.40	2.82
TiO ₂	0.76	0.83	0.82	0.50	0.50
P ₂ O ₅	0.14	0.14	0.14		0.14
LOI	1.82	1.92			
Tot	98.94	99.17	100.00	100.35	99.03
ppm					
Sc	16	17	16	11	16
Be*	2	3	2	3	
V*	100	109	104	60	109
Co	14	16	15	10	16
Ni*	32	34	33	20	29
Cu*	13	14	14	25	
Zn*	80	90	85	71	
Ga	23	24	24	17	
Ge	1.6	1.6	1.6	1.6	
Rb	144	130	137	112	89
Sr	119	132	126	350	262
Y	28	29	28	22	30
Zr	181	201	191	190	168
Nb	12	12	12	25	12
Sn*	3	3	3	5.5	
Cs	4.1	4.2	4.2	3.7	
Ba	551	620	586	550	683

TABLE 4: *Continued*

	Sila nappe section A-A'	Sila nappe section B-B'	av. anhydrous composition	upper crust ¹	upper crust ²
ppm					
La	37.43	42.29	39.86	30	25.4
Ce	72.68	81.65	77.16	64	56.8
Pr	8.16	9.13	8.64	7.1	
Nd	31.79	35.48	33.64	26	26
Sm	6.37	6.94	6.66	4.5	4.97
Eu	1.19	1.32	1.26	0.88	1.02
Gd	5.68	6.12	5.90	3.8	4.71
Tb	0.83	0.87	0.85	0.64	0.74
Dy	4.79	4.98	4.88	3.5	
Ho	0.94	0.97	0.96	0.8	
Er	2.79	2.90	2.84	2.3	
Tm	0.41	0.43	0.42	0.33	
Yb	2.54	2.62	2.58	2.20	2.29
Lu	0.38	0.39	0.38	0.32	0.38
Σ REE	175.98	196.10	186.04	146.37	146.37
Hf	5.2	5.6	5.4	5.8	4.4
Ta	1.2	1.1	1.2	2.2	0.90
Tl	0.92	0.87	0.90	0.75	
Pb*	14	14	14	20	16
Th	14.0	15.5	14.8	10.70	8.9
U	2.74	2.70	2.72	2.80	2.4
Th/U	5.1	5.8	5.45	3.8	3.7
A**	2.06	2.13	2.10	1.83	1.54

¹ Taylor e McLennan (1985). ² Condie (1993). * below detection limits in some samples. ** radiogenic heat production; decay energies from Philpotts (1990); density = 2800 kg/m³.

partially precluding their transfer to melt; thus REE and Th remained in large amounts in the residue (see Bea *et al.*, 1994; Harris *et al.*, 1995; Nabelek and Glascock, 1995; Bea, 1996).

Only when temperatures were high enough to promote biotite breakdown, accessory phases and consequently REE and Th could be released into the melts. Interestingly, the garnet-cordierite fels which only contains a little biotite, is characterised by lower contents of REE. Here, biotite breakdown probably favoured transfer of REE-bearing accessory phases to the melts.

CONSIDERATIONS ON INTRACRUSTAL DIFFERENTIATION IN SILA NAPPE

The metasedimentary rocks of the upper crust show minor compositional modifications from a typical pelitic or arenitic protolith, whereas comparisons between the metasedimentary rocks above and below the granitoids reveal important changes. Considering major oxides, higher Al₂O₃, Fe₂O₃*, MgO and TiO₂ and lower SiO₂ are observed in the migmatitic paragneiss. In relation to trace elements, higher contents of REE, Zr and Th are detected in most of the

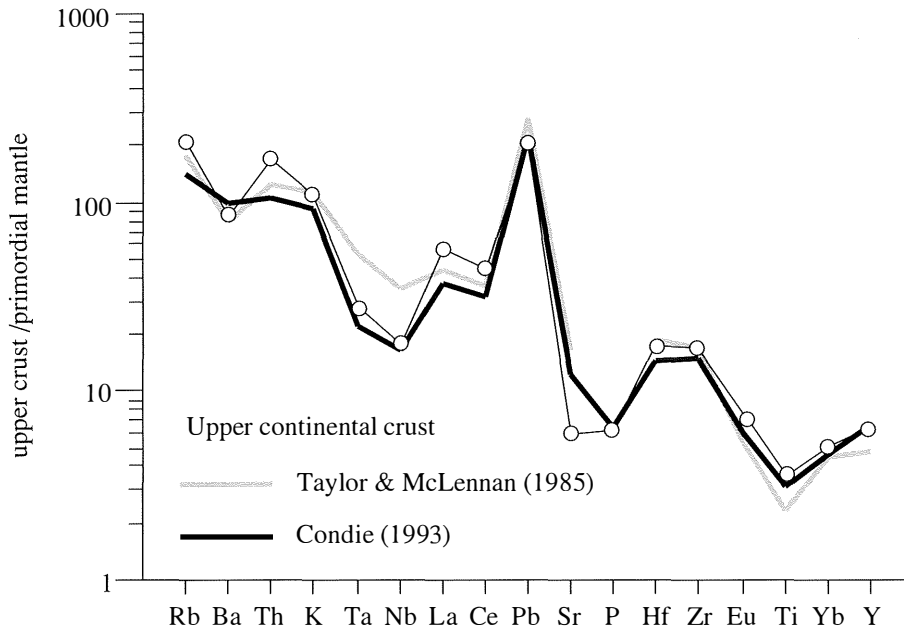


Fig. 13 ~ Incompatible elements spider-diagram showing comparisons between weighted average compositions of Sila nappe and estimates of upper continental crust composition, from Taylor and McLennan (1985) and Condie (1993). Primitive mantle normalising values from Sun and McDonough (1989).

migmatitic paragneiss. These variations cannot be ascribed only to original compositional differences. Extreme concentrations observed in some migmatitic paragneiss should mainly be attributed to the effects of crustal anatexis by muscovite dehydration melting. Biotite remained mostly stable through melting reactions and armoured accessory phases such as monazite and zircon. The positive covariation of K_2O and Ce in fig. 8b confirms enrichment in biotite and monazite in the residue. Thus, in migmatite, moderate amounts of K and U and high Th imply an increase in radiogenic heat production in the lower level of the crustal section in question. This finding means that the isobaric cooling recorded in the high-grade rocks of the Sila nappe (Gräßner, 1999) cannot be connected with upward migration of U, Th and K with anatectic melts (see Philpotts, 1990; Bohlen, 1991).

Of the granitoid rocks, leucogranite displays low Sr and Ba and high Rb, which probably

excludes an origin by differentiation from the other granitoids (see Rb and Ba diagrams of fig. 10). Their geochemical characteristics may be linked to an origin by partial melting of a metapelitic source rock. Anatectic melts with low proportions of plagioclase can form by muscovite dehydration reactions. A composition characterised by low Sr and Ba and high Rb (Rb/Sr ratio > 5), similar to Himalayan leucogranite, may be produced by fluid-absent melting (Harris *et al.*, 1995; Patiño Douce and Harris, 1998). In addition, the low Zr, REE and Th of the Sila leucogranite counter-balance the Zr, REE and Th enrichment observed in the migmatitic paragneiss. Direct connection of leucogranite genesis with anatexis of the Sila medium- to high-grade metapelite is, however, difficult to ascertain: the leucogranite probably underwent later evolution by feldspars fractionation, as indicated by the pronounced negative Eu spike.

Leucogranodiorite sample BOC 78,

characterised by very high Sr and Ba, low Rb, and a REE pattern with negligible Eu anomaly, confirms that the genesis of the Sila granitoids is complex. For genesis by partial melting of metapelite, the compositional features of the leucogranodiorite require the conspicuous involvement of plagioclase and a lower proportion of micas. Experimental work carried out by Patiño Douce and Harris (1998) demonstrates that granitoid melts with a high proportion of plagioclase and an Rb/Sr ratio < 2 may be produced by H₂O fluxing of a metapelitic source. Thus, partial melting of the intermediate-crust metapelite probably took place in different ways, involving H₂O availability and extensive involvement of muscovite or plagioclase. These considerations suggest that specific studies are needed for quantitative examination of the connection between partial melting of metapelite and granite genesis in the Sila crustal section.

CONCLUDING REMARKS

The observation of the Late Hercynian section through the upper and intermediate continental crust exposed in the Sila nappe suggests a simple three-level structure. This includes: 1) upper level: low- to medium-grade metapelite to meta-arenite with minor marble and meta-volcanic rocks; 2) intermediate level: granitoids with composition varying from tonalite to leucogranite; 3) lower level: migmatitic paragneiss with minor metabasite.

The thickness of the granitoids, estimated on cross-sections and checked by geobarometry, is 9 ± 2 km.

Estimates of bulk composition are strongly affected by the elevated amount of metapelite. Consequently, high Al₂O₃, REE and Th and low CaO and Sr are detected. In addition, negative Eu anomalies in REE patterns are observed in most rock types, fitting the composition of typical post-Archean upper crust (Taylor and McLennan, 1985; Condie, 1993).

Comparisons between upper and

intermediate metapelites indicate important compositional differences, chiefly attributed to intracrustal differentiation through partial melting of intermediate-crust metapelite. Muscovite dehydration melting reactions determined enrichment of Al₂O₃, Fe₂O₃*, MgO and TiO₂, and of REE, Th and Zr in the residue. The increase in REE and Th is considered to depend closely on the behaviour of monazite which, during melting reactions, generally remained in the residue, armoured by biotite.

Radiogenic heat production, calculated from the abundances of Th, U and K, increases from upper to intermediate metasedimentary rocks. This trend appears to be related to the distribution of monazite and biotite.

Compositions similar to those of the Sila leucogranite, characterised by low Ba and Sr and high Rb, may be obtained by muscovite dehydration melting reactions from a metapelitic source. In the Sila nappe, the genesis of the leucogranite appears to be connected with intracrustal differentiation.

ACKNOWLEDGMENTS

Helpful comments by Alessandro Borghi and Jörn H. Kruhl are gratefully acknowledged. The research was financially supported by Univ. Basilicata funds, linked to MURST project «A model for the geochemical and petrographic composition of the continental crust in selected Italian sites».

REFERENCES

- ACQUAFREDDA P., BARBIERI M., LORENZONI S., TRUDU C. and ZANETTIN LORENZONI E. (1991) — *The age of volcanism and metamorphism of the Bocchigliero Paleozoic sequence (Sila, Southern Italy)*. Rend. Fis. Acc. Lincei, **2**, 145-156.
- ACQUAFREDDA P., BARBIERI M., LORENZONI S., TRUDU C. and ZANETTIN LORENZONI, E. (1992a) — *Metamorphism of the Mandatoriccio Unit in the context of the Hercynian and pre-Hercynian evolution of the Calabrian-Peloritan Arc (Southern Italy)*. Rend. Fis. Acc. Lincei, **3**, 151-161.
- ACQUAFREDDA P., CAGGIANELLI A. and PICCARRETA G. (1992b) — *Late magmatic to subsolidus*

- coronas in gabbroic rocks from the Sila massif, Calabria, Italy. *Mineral. Petrol.*, **46**, 229-238.
- ACQUAFREDDA P., LORENZONI S. and ZANETTIN LORENZONI E. (1994) — *Palaeozoic sequences and evolution of the Calabrian-Peloritan Arc, Southern Italy*. Terra Nova, **6**, 582-594.
- ALVAREZ W. (1976) — *A former continuation of the Alps*. *Geol. Soc. Am. Bull.*, **87**, 891-896.
- AMODIO-MORELLI L., BONARDI G., COLONNA V., DIETRICH D., GIUNTA G., IPPOLITO F., LIGUORI V., LORENZONI S., PAGLIONICO A., PERRONE V., PICCARRETA G., RUSSO M., SCANDONE P., ZANETTIN-LORENZONI E. and ZUPPETTA A. (1976) — *L'Arco Calabro-Peloritano nell'orogene Appenninico - Maghrebide*. *Mem. Soc. Geol. It.*, **17**, 1-60.
- ANDERSON J.L. and SMITH D.R. (1995) — *The effects of temperature and oxygen fugacity on the Al-in-hornblende barometer*. *Am. Mineral.*, **80**, 549-559.
- AYUSO R.A., MESSINA A., DE VIVO B., RUSSO S., WOODRUFF L.G., SUTTER J.F. and BELKIN H.E. (1994) — *Geochemistry and argon thermochronology of the Variscan Sila batholith, southern Italy: source rocks and magma evolution*. *Contrib. Mineral. Petrol.*, **117**, 87-109.
- BARTH M.G., McDONOUGH W.F. and RUDNICK R.L. (2000) — *Tracking the budget of Nb and Ta in the continental crust*. *Chem. Geol.*, **165**, 197-213.
- BEA F. (1996) — *Residence of REE, Y, Th and U in granites and crustal protoliths; implications for the chemistry of crustal melts*. *J. Petrol.*, **37**, 521-552.
- BEA F., PEREIRA M.D. and STROH A. (1994) — *Mineral/leucosome trace-element partitioning in a peraluminous migmatite (a laser ablation-ICP-MS study)*. *Chem. Geol.*, **117**, 291-312.
- BOHLEN S.R. (1991) — *On the formation of granulites*. *J. Metamorphic Geol.*, **9**, 223-229.
- BONARDI G., CAVAZZA W., PERRONE V. and ROSSI S. (in press) - *Calabria-Peloritani terrane and northern Ionian Sea*. In: Martini I.P. and Vai G.B. (Eds.): *Anatomy of a Mountain Chain: the Apennines and Adjacent Mediterranean Basins*. Chapman e Hall, London.
- BORCHI A., COLONNA V. and COMPAGNONI R. (1992) — *Structural and metamorphic evolution of the Bocchigliero and the Mandatoriccio complexes in the Sila Nappe Calabrian-Peloritan Arc, southern Italy*. In: Carmignani L. and Sassi F.P. (Eds.): «Contributions to the Geology of Italy with special regard to the Paleozoic basements». IGCP, **276** (5), 321-334.
- BOUNDY T.M., ESSENE E.J., HALL C.M., AUSTRHEIM H. and HALLIDAY A.N. (1996) — *Rapid exhumation of lower crust during continent-continent collision and late extension: evidence from $^{40}\text{Ar}/^{39}\text{Ar}$ incremental heating of hornblendes and muscovites, Caledonian orogen, western Norway*. *Geol. Soc. Am. Bull.*, **108**, 1425-1437.
- BURTON A.N. (1971) — *Carta geologica della Calabria alla scala 1:25000*. Relazione generale, Cassa per il Mezzogiorno, I.G.M., Firenze, 120 p.
- CAGGIANELLI A., DEL MORO A., PAGLIONICO A., PICCARRETA G., PINARELLI L. and ROTTURA A. (1991) — *Lower crustal granite genesis connected with chemical fractionation in the continental crust of Calabria, Southern Italy*. *Eur. J. Mineral.*, **3**, 159-180.
- CAGGIANELLI A., DEL MORO A. and PICCARRETA G. (1994) — *Petrology of basic and intermediate orogenic granitoids from the Sila massif Calabria, southern Italy*. *Geol. J.*, **29**, 11-28.
- CAGGIANELLI A., PROSSER G. and DI BATTISTA P. (1997) — *Textural features and fabric analysis of granitoids emplaced at different depths: the example of the Hercynian tonalites and granodiorites from Calabria*. *Mineral. Petrol. Acta*, **40**, 11-26.
- CLARKE D.B. (1992) — *Granitoid Rocks*. Chapman and Hall, London, 283 pp.
- CONDIE K.C. (1989) — *Plate Tectonics and Crustal Evolution*. Pergamon Press, Oxford, 476 pp.
- CONDIE K.C. (1993) — *Chemical composition and evolution of the upper continental crust: contrasting results from surface samples and shales*. *Chem. Geol.*, **104**, 1-37.
- DUBOIS R. (1971) — *Définition d'un socle antéhercynien en Calabre*. *C.R. Acad. Sci. Paris*, **272**, 2050-2055.
- DUBOIS R. (1976) — *La suture calabro-apenninique crétacé-éocène et l'ouverture Tyrrhénienne néogène: étude pétrographique et structurale de la Calabre centrale*. Thèse Université P. et M. Curie, 567 pp.
- ELLIS D.J. (1987) — *Origin and evolution of granulites in normal and thickened crust*. *Geology*, **15**, 167-170.
- EMMERMANN R. and SCHENK V. (1989) — *Chemical differentiation of continental crust in southern Calabria*. Abstract volume from Varallo conference on the lower continental crust, 32-33.
- FOUNTAIN D.M. and SALISBURY M.H. (1981) — *Exposed cross-sections through the continental crust: implications for crustal structure, petrology and evolution*. *Earth Planet. Sci. Lett.*, **56**, 263-277.
- GRÄBNER T. (1999) — *Thermal evolution of the continental crust of Calabria during the Hercynian orogeny: constraints from metamorphic phase equilibria and isotopic dating*. Ph.D. thesis, University of Kiel, 108 pp.
- GRÄBNER T., SCHENK V., BRÖCKER M. and MEZGER K. (2000) — *Geochronological constraints on the timing of granitoid magmatism, metamorphism*

- and post-metamorphic cooling in the Hercynian crustal cross-section of Calabria. *J. Metamorphic Geol.*, **18**, 409-421.
- HARRIS N., AYRES M. and MASSEY J. (1995) — *Geochemistry of granitic melts produced during the incongruent melting of muscovite: implications for the extraction of Himalayan leucogranite magmas*. *J. Geophys. Res.*, **100** B8, 15767-15777.
- HERRON M.M. (1988) — *Geochemical classification of terrigenous sands and shales from core or log data*. *J. Sed. Petrol.*, **58**, 820-829.
- HOLDAWAY M.J. (1971) — *Stability of andalusite and aluminum silicate phase diagram*. *Am. J. Sci.*, **271**, 97-131.
- HOLLAND T.J.B. and BLUNDY J. (1994) — *Non-ideal interactions in calcic amphiboles and their bearing on amphibole-plagioclase thermometry*. *Contrib. Mineral. Petrol.*, **116**, 433-447.
- HOLLAND T.J.B. and POWELL R. (1998) — *An internally-consistent thermodynamic data set for phases of petrological interest*. *J. Metamorphic Geol.*, **16**, 309-344.
- IRVINE T.N. and BARAGAR W.R.A. (1971) — *A guide to the chemical classification of the common volcanic rocks*. *Canad. J. Earth Sci.*, **8**, 523-548.
- LORENZONI S. and ZANETTIN LORENZONI E. (1983) — *Note illustrative della Carta Geologica della Sila alla scala 1:200000*. *Mem. Sci. Geol.*, Padova, **36**, 317-342.
- LUX D.R., DEYOREO J.J., GUIDOTTI C.V. and DECKER E.R. (1986) — *Role of plutonism in low-pressure metamorphic belt formation*. *Nature*, **323**, 794-797.
- MCDONOUGH W.F. and SUN S.-s. (1995) — *The composition of the Earth*. *Chem. Geol.*, **120**, 223-253.
- MCLENNAN S.M. (1989) — *Rare earth elements in sedimentary rocks: influence of provenance and sedimentary processes*. In: B.R. Lipin and G.A. McKay (Eds.), *Geochemistry and Mineralogy of Rare Earth Elements*. *Am. Mineral. Soc. Rev. Mineral.*, **21**, 169-200.
- NABELEK P.I. and GLASCOCK D. (1995) — *REE-depleted leucogranites, Black Hills, South Dakota: a consequence of disequilibrium melting of monazite-bearing schists*. *J. Petrol.*, **36**, 1055-1071.
- NICHOLS G.T., BERRY R.F. and GREEN D.H. (1992) — *Internally consistent garnitic spinel-cordierite-garnet equilibria in the FMShZn system: geothermobarometry and applications*. *Contrib. Mineral. Petrol.*, **111**, 362-377.
- PATIÑO DOUCE A.E. and HARRIS N. (1998) — *Experimental constraints on Himalayan anatexis*. *J. Petrol.*, **39**, 689-710.
- PATTISON D.R.M. and TRACY R.J. (1991) — *Phase equilibria and thermobarometry of metapelites*. In: Kerrick, D.M., ed.: *Contact metamorphism*. *Mineral. Soc. Am., Washington D.C.*, **26**, 105-206.
- PERCIVAL J. (1988) — *Deep geology out in the open*. *Nature*, **335**, 671.
- PHILPOTTS A.R. (1990) — *Principles of igneous and metamorphic petrology*. Englewood Cliffs, Prentice Hall, 498 pp.
- PICCARRETA G. (1972) — *Presenza di lawsonite e pumpellyite negli scisti verdi affioranti tra il Monte Reventino e Falerna (Calabria)*. *Per. Mineral.*, **41**, 153-161.
- RUDNICK R.L. (1995) — *Making continental crust*. *Nature*, **378**, 571-578.
- SCHENK V. (1981) — *Synchronous uplift of the lower crust of the Ivrea Zone and of southern Calabria and its possible consequences for the Hercynian orogeny in southern Europe*. *Earth Planet. Sci. Lett.*, **56**, 305-320.
- SCHENK V. (1989) — *P-T-t path of the lower crust in the Hercynian fold belt of Southern Calabria*. In: Daly J.S., Cliff R.A. and Yardley B.W.D. (Eds.): *Evolution of metamorphic belts*. *Geol. Soc. Spec. Publ.*, **43**, 337-342.
- SENESI G.S. (1999) — *Petrologia della zona di bordo delle plutoniti nelle Serre, Catanzaro, Calabria*. PhD thesis, Bari University, 80 pp.
- SPEAR F.S. (1993) — *Metamorphic phase equilibria and pressure-temperature-time paths*. *Mineral. Soc. Am., Washington D.C.*, 799 pp.
- SUN S. and MCDONOUGH W.F. (1989) — *Chemical and isotopic systematics of oceanic basalts: implications for mantle composition and processes*. In: Saunders, A.S. and Norry, M.J., eds.: *Magmatism in ocean basins*. *Geol. Soc. Lond. Spec. Publ.*, **42**, 313-345.
- TAYLOR S.R. and MCLENNAN S.M. (1985) — *The continental crust: its composition and evolution*. Oxford, Blackwell, 312 pp.
- THOMSON S.N. (1994) — *Fission track analysis of the crystalline basement rocks of the Calabrian Arc, southern Italy: evidence of Oligo-Miocene late-orogenic extension and erosion*. *Tectonophysics*, **238**, 331-352.
- VAN DIJK J.P., BELLO M., BRANCALEONI G.P., CANTARELLA G., COSTA V., FRIXA A., GOLFETTO F., MERLINI S., RIVA M., TORRICELLI S., TOSCANO C. and ZERILLI A. (2000) — *A regional structural model for the Northern Sector of the Calabrian Arc, Southern Italy*. *Tectonophysics*, **324**, 267-320.
- WATT G.R., BURNS I.M. and GRAHAM G.A. (1996) — *Chemical characteristics of migmatites: accessory phase distribution and evidence for fast melt segregation rates*. *Contrib. Mineral. Petrol.*, **125**, 100-111.

